

# Engineered Synthetic Polymer Nanoparticles as IgG Affinity Ligands

Shih-Hui Lee,<sup>†,§</sup> Yu Hoshino,<sup>‡</sup> Arlo Randall,<sup>¶,⊥</sup> Zhiyang Zeng,<sup>†</sup> Piere Baldi,<sup>¶,⊥</sup> Ruey-an Doong,<sup>§</sup> and Kenneth J. Shea<sup>\*,†</sup>

<sup>†</sup>Department of Chemistry, University of California, Irvine, Irvine, California 92697, United States

<sup>‡</sup>Department of Chemical Engineering, Kyushu University, Motooka, Fukuoka 819-0395, Japan

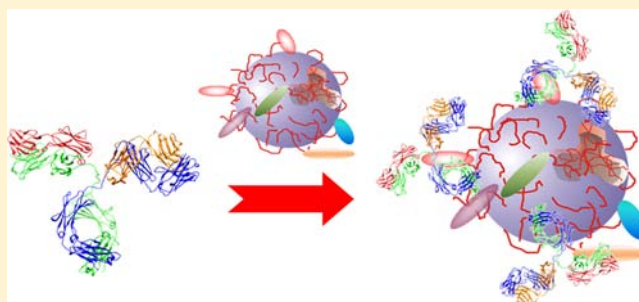
<sup>§</sup>Department of Biomedical Engineering and Environmental Sciences, National Tsing Hua University, Hsinchu, 30013, Taiwan

<sup>¶</sup>Department of Computer Science, University of California, Irvine, Irvine, California 92697, United States

<sup>⊥</sup>Institute for Genomics and Bioinformatics, University of California, Irvine, Irvine, California 92697, United States

## Supporting Information

**ABSTRACT:** A process for the preparation of an abiotic protein affinity ligand is described. The affinity ligand, a synthetic polymer hydrogel nanoparticle (NP), is formulated with functional groups complementary to the surface presentation of the target protein. An iterative process is used to improve affinity by optimizing the composition and proportion of functional monomers. Since the polymer NPs are formed by a kinetically driven process, the sequence of functional monomers in the polymer chain is not controlled; only the average composition can be adjusted by the stoichiometry of the monomers in the feed. To compensate for this the hydrogel NP is lightly cross-linked resulting in chain flexibility that takes place on a submillisecond time scale allowing the polymer to “map” onto a protein surface with complementary functionality. In this study, we report a lightly cross-linked (2%) *N*-isopropyl acrylamide (NIPAm) synthetic polymer NP (50–65 nm) incorporating hydrophobic and carboxylate groups that binds with high affinity to the Fc fragment of IgG. The affinity and amount of NP bound to IgG is pH dependent. The hydrogel NP inhibits protein A binding to the Fc domain at pH 5.5, but not at pH 7.3. A computational analysis was used to identify potential NP–protein interaction sites. Candidates include a NP binding domain that overlaps with the protein A–Fc binding domain at pH 5.5. The computational analysis supports the inhibition experimental results and is attributed to the difference in the charged state of histidine residues. Affinity of the NP (3.5–8.5 nM) to the Fc domain at pH 5.5 is comparable to protein A at pH 7. These results establish that engineered synthetic polymer NPs can be formulated with an intrinsic affinity to a specific domain of a large biomacromolecule.



## INTRODUCTION

Nanomedicine is driven by the premise that discrete synthetic nanoparticles (NPs) can be formulated to target specific proteins, cells, or organs. NP targeting coupled with function (drug delivery, imaging, diagnostics, concentration, isolation, and purification) provides opportunities for transformative approaches to therapeutics, diagnostics, and biomacromolecule isolation and purification. This is a vibrant area of research with recent successes that include therapeutic reagents,<sup>1,2</sup> drug delivery vehicles,<sup>3–5</sup> sensors,<sup>6–8</sup> toxin neutralization,<sup>9–11</sup> and enzyme inhibition.<sup>12,13</sup> NP specificity for target biomolecules is most often accomplished by the attachment of affinity ligands, including antibodies. The need for a comprehensive collection of affinity agents for proteins has been heightened by the National Institutes of Health’s (NIH’s) broad initiative to obtain multiple capture agents for all proteins in the proteome.<sup>14</sup>

Recombinant antibodies are the current gold standard of affinity agents and it is likely they will play a dominant role for

the foreseeable future. However, antibodies are not without some limitations. For example, the cost of developing new protein capture agents is high. The time required for discovery of an effective antibody can also be lengthy. Some proteins may not function for all intended applications. These and related issues create practical challenges to formulating a comprehensive set of antibody target capture reagents. In addition to antibodies, alternative technologies that include peptides, peptide mimics, and aptamers offer promising opportunities to expand the candidate pool of protein capture reagents.<sup>15–17</sup> Considering the range of targets and uses, it is likely that a combination of approaches will be needed to generate a comprehensive resource.

We have been developing an alternative approach for protein and peptide capture agents. Our strategy takes cognizance of the fact that protein–protein interaction surfaces span

Received: April 15, 2012

Published: August 27, 2012

hundreds of square angstroms.<sup>18</sup> Affinity arises from the cumulative effect of individually weak interactions that include van der Waals, hydrogen bonding, and electrostatic interactions. Our capture agent, a synthetic polymer hydrogel, is formulated with functional groups complementary to protein domains or peptide targets. We then use an iterative process to improve affinity to a target peptide or protein by optimizing the composition and proportion of functional monomers. Since the polymer NPs are formed by a kinetically driven process, the sequence of functional monomers in the polymer chain is not controlled; only the average composition of the polymer can be adjusted by the stoichiometry of the monomers in the feed. However, to compensate for this the hydrogel NP is lightly cross-linked (~2%) resulting in considerable chain flexibility that takes place on a submillisecond time scale.<sup>19</sup> This allows the polymer to “map” onto a protein surface with complementary functionality compensating in part for the lack of sequence and topological control of the synthetic polymer NP.

Our previous efforts focused on synthetic polymer NPs with antibody-like affinity and selectivity to a toxic peptide, melittin. Polymer NPs with low nanomolar affinity and high selectivity were developed and were shown to function by neutralizing the peptides toxicity in vitro and in vivo.<sup>10,20</sup> The present study describes an important step beyond peptide recognition and capture, specifically, progress in developing a synthetic polymer NP that binds to a specific targeted domain of a large protein.

The protein target of this study is the 150 kDa protein immunoglobulin G (IgG). IgG is the workhorse protein for research, diagnostics, and increasingly, therapeutic applications.<sup>21,22</sup> IgGs are composed of 4 protein chains, 2 identical heavy chains of approximately 50 kDa and 2 identical light chains of about 25 kDa. The tetramer has two identical halves that form a forked Y shape. Each end of the fork contains an identical antigen-binding site (the variable regions). The structure is given in Figure 1, which also highlights heavy and

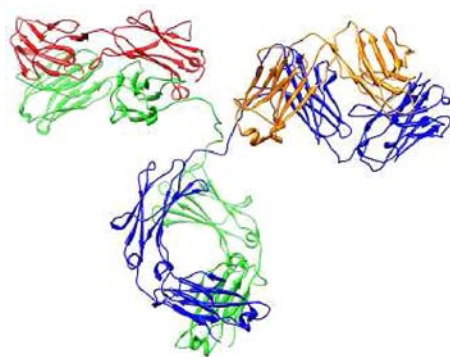


**Figure 1.** The structure of IgG with heavy chains in blue and green and light chains in orange and red. The Fc–Fc dimer is shown at the bottom of the image. The PDB ID is 1HZH.

light chains. The base or conserved region of the structure corresponds to the Fc fragment (Figure 1) and can be cleaved from IgG and studied independently. Purification of recombinant IgG from cellular extract is often achieved by a multistep process that includes chromatographic separation using protein affinity ligands that strongly and specifically bind to the conserved Fc domain. Protein A or G are the most common affinity ligands used for purification of IgG. Protein A and G themselves are products of recombinant technology and must

be expressed and purified. It is not surprising therefore that considerable effort has been expended in the design of alternatives to protein A/G. These alternatives have included synthetic ligands,<sup>22,23</sup> DNA/RNA aptamers,<sup>16</sup> peptides,<sup>15,17</sup> and synthetic polymers.<sup>24,25</sup> The utility of the Fc domain as a target for protein capture dictated its choice for our study.

A small library of multifunctional polymer NPs containing varying amounts of hydrophobic, hydrophilic, and charged monomers were screened for IgG affinity and the “hits” were taken into a second round of NP synthesis, tuning the composition of critical monomers to arrive at NPs with high affinity for IgG. A more focused effort followed to establish that the dominant NP–protein interaction is with the Fc domain of IgG. This effort was coupled with analysis of the Fc protein surface to identify potential Fc–NP binding domains and their response to changes in pH. Finally a NP–protein A competition was performed to help identify the location of the dominant NP–IgG interaction.

## RESULTS AND DISCUSSION

**Synthesis and Screening of NP–IgG Affinity.** A small library of multifunctional hydrogel NPs (NP1–6) were synthesized by precipitation polymerization.<sup>10,26,27</sup> *N*-isopropyl acrylamide (NIPAm) was the core monomer in combination with various amounts of acrylic acid (AAc), *N*-(3-aminopropyl) methacrylamide hydrochloride (APM), and *N*-*t*-butyl acrylamide (TBAm), as negatively charged, positively charged and hydrophobic functional monomers, respectively. *N,N'*-Methylene-bis-acrylamide (Bis, 2 mol %) was incorporated as a cross-linker (Figure 2). NP size was established by dynamic light

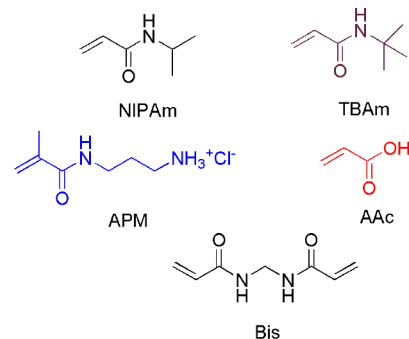


**Figure 2.** Monomers used for NP synthesis.

scattering (DLS, Table 1). Table S1 in the Supporting Information summarizes the feed ratio and reaction conditions used to prepare the NP library. DLS was also used in the initial screen of NP–IgG interactions in water.<sup>28,29</sup> An association between a NP and IgG (10–12 nm)<sup>28</sup> should result in an observable increase in particle size. From this screen, NP6 incorporating both TBAm and AAc monomers showed a significant increase in size following addition of IgG (Table 1). NP1 and NP4 also exhibited an increase in size upon addition of IgG.

The interactions of NP1, NP4, and NP6 with Fc-orientated IgG were evaluated by QCM (quartz crystal microbalance) in PBS (35 mM, pH 7.3 with 150 mM NaCl). IgG orientation was achieved by first immobilizing its antigen, TNF $\alpha$  (tumor necrosis factor- $\alpha$  human), on the QCM surface. The surface was then functionalized with humanized monoclonal IgG (anti-TNF $\alpha$  antibody).<sup>30</sup> Since TNF $\alpha$  binds the Fab fragment of IgG, this orientates the Fc domain into the bulk solution

**Table 1. Composition, Yield, and Diameter of NPs in Pure Water in the Absence/Presence of IgG (133 nM) in Water**

NP no.	feed ratio of functional monomers [%] <sup>a</sup>			yield [%]	diameter [nm] <sup>b</sup>	diameter after the addition of IgG [nm] <sup>c</sup>
	TBAAm	APM	AAc			
1	40	0	0	61.6	56	aggregation <sup>d</sup>
2	0	5	0	30.1	94	89
3	0	0	5	84.1	20	20
4	0	0	0	87.7	88	105
5	40	5	0	26.4	110	110
6	40	0	5	64.0	60	aggregation <sup>d</sup>
7	40	0	20	65.2	64	aggregation <sup>d</sup>
8	40	0	40	48	58	aggregation <sup>d</sup>

<sup>a</sup>NIPAm is present according to the following relationship (NIPAm = 98 – TBAAm – APM – AAc). In all cases, Bis is present as 2% of the total monomer composition. <sup>b</sup>Average of at least 3 independent measurements (standard deviation 0.2 to 1.9 nm). <sup>c</sup>Average of at least 3 independent measurements (standard deviation 0.1 to 2.1 nm). <sup>d</sup>Aggregation is defined by the observation of polymodality with formation of micrometer-sized species.

making it accessible to NPs. A 0.1% BSA (bovine serum albumin) solution was subsequently added to reduce non-specific binding. To confirm the Fc domain was accessible from solution, the prepared surface was exposed to Au NPs coated with an anti-human IgG that specifically binds to the Fc domain of IgG. The strong signal confirmed that the Fc domain was accessible to solution affinity ligands (Figure S1, Supporting Information), validating the use of this method to screen NP affinity for the Fc domain of IgG. The binding of NP1, NP4, and NP6 to the oriented IgG is summarized in Figure 3. NP6

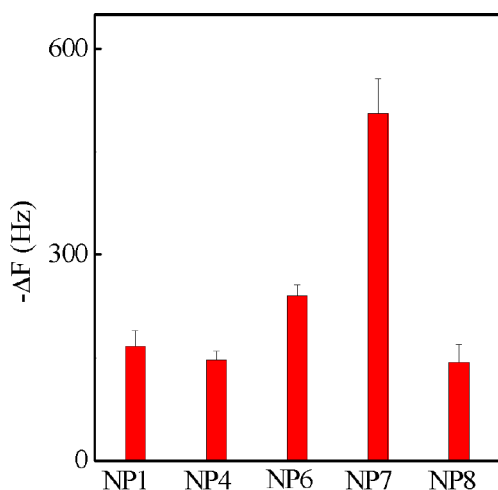


**Figure 3.** QCM screening of the library of polymer NPs containing 40% TBAAm and varying amounts of AAc with Fc-oriented IgG in PBS (35 mM, pH 7.3 with 150 mM NaCl). Standard deviations were calculated from three independent measurements.

showed greater frequency change than NP1 and NP4. The NPs are comprised of functional groups that could participate in hydrogen bonding, hydrophobic and electrostatic interactions with proteins. This preliminary result suggests that a combination of these functional groups is necessary for binding.

**Optimization of NP Composition and Evaluation of NP Binding Specificity.** In an effort to maximize NP affinity

to IgG, an expanded pool of NPs was prepared. One series contained greater amounts of AAc than NP6 (NP7 and NP8, Table 1 and S2, Supporting Information). However, efforts to prepare NPs with greater amounts of TBAAm were not successful due to the colloidal instability of the resulting materials. The binding of NP1, NP6, NP7, and NP8 to the oriented IgG is summarized in Figure 3. The frequency change of NP7 (20% AAc, 40% TBAAm) was two to three times higher than that of other NPs. This NP was taken on for further experiments.

In addition to IgG affinity a preliminary screen for protein specificity was undertaken. The interaction of BSA, TNF $\alpha$ , and hemoglobin against NP7 was studied in PBS (35 mM, pH 7.3 with 150 mM NaCl). NP7 had little interaction with these proteins (Figure 4), suggesting that in the above diagnostic, the

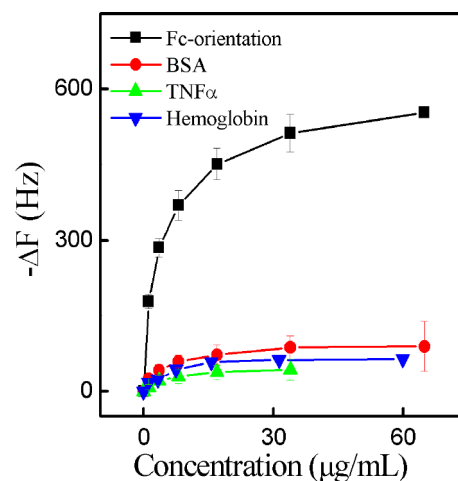


**Figure 4.** The interactions between NP7 and IgG, BSA, TNF $\alpha$  and hemoglobin each of which were immobilized on a QCM surface in PBS (35 mM, pH 7.3 with 150 mM NaCl). Standard deviations were calculated from three independent measurements.

observed NP affinity for IgG was primarily associated with the oriented Fc domain of IgG. In addition, multivalency of the interaction between NP7 and IgG was established by observing changes in particle size by DLS before and after the addition of IgG to an aqueous solution of NPs. At a molar ratio of IgG to NP of 1.25, aggregates formed (Figure S2, Supporting Information). We interpret this observation as multivalency of both IgG and the NPs.

#### Effect of pH and Buffer on NP–Protein Interactions.

The preceding experiments provided evidence for a strong interaction between NP7 with the Fc domain of IgG. The composition of protein and functional polymer NP surfaces renders these interactions susceptible to binding conditions such as pH and ionic strength. The response to these variables can provide information about the nature of the binding.<sup>31–35</sup> The influences of pH and ionic strength on the NP7–Fc interaction are summarized in Figure 5. In phosphate buffer (pH 7.3, without NaCl), an increase in phosphate concentration from 2 mM to 35 mM resulted in a 3-fold increase in the amount of protein bound to NP7 (Figure 5a, note that pH of the solution did not change even in the low buffer concentration). This implies that under the specified conditions the dominant contribution to binding is from hydrophobic interactions.<sup>32</sup> A comparison of parts a and b of Figure 5 reveals the binding between the Fc domain and NP7 is at least twice as

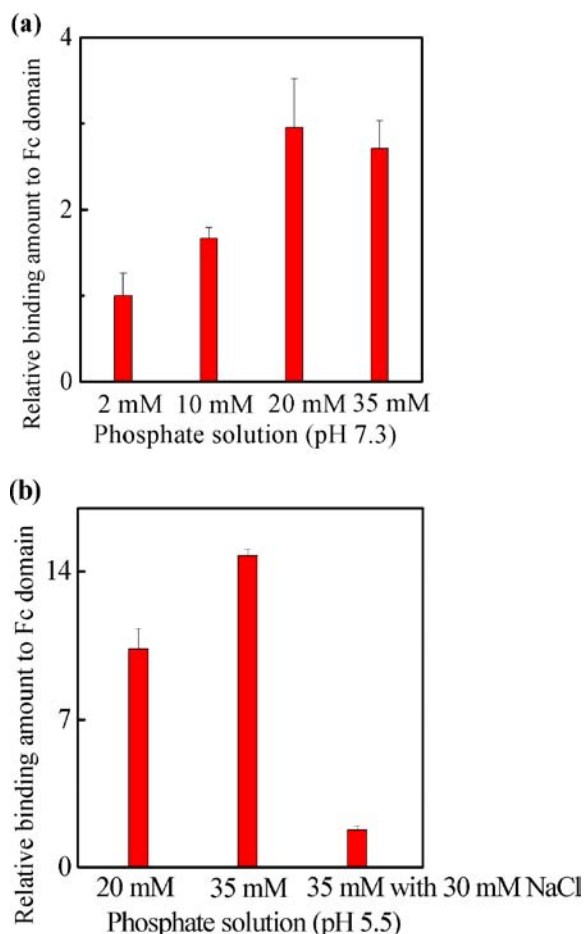


**Figure 5.** The interaction between the Fc domain and NP7 by QCM at various phosphate concentrations at (a) pH 7.3 and (b) pH 5.5. The relative amount is related to the amount of NP7 bound to the Fc domain at various salt concentrations compared to the amount bound in 2 mM phosphate buffer at pH 7.3. Standard deviations were calculated from three independent measurements.

strong at pH 5.5 than at pH 7.3 in 20 mM phosphate buffer (without NaCl). At pH 7.3, exposed lysine ( $pK_a = 10.79$ ) and arginine residues ( $pK_a = 12.48$ ) are positively charged but at pH 5.5 and below histidine ( $pK_a = 6.04$ ) is also positively charged. A mixture composed mainly of IgG1 and IgG2 is used in these studies. Assuming the five exposed histidine residues on the Fc domain are positively charged at or below pH 5.5, the human IgG1 Fc domain is estimated to have a net charge of +1 at neutral pH but +6 at or below pH 5.5 (see Table S3, Supporting Information). Similarly, the human IgG2 Fc domain has a net charge of 0 at neutral pH, but a net charge of +6 at or below pH 5.5. On the basis of simple electrostatic arguments, NP7 is expected to have a stronger interaction for the Fc domain at pH 5.5. Some support for this comes from the effect of ionic strength on binding. It was noted that the binding amount at pH 5.5 decreased as the NaCl salt concentration of 35 mM phosphate buffer was raised from 0 mM to 30 mM. This response is typical of a binding with contributions from electrostatic interactions.<sup>34,35</sup>

**Inhibition of Protein A–Fc Binding by NP7.** Protein A binds to the Fc domain of IgG. This strong and specific affinity is utilized for antibody purification. An X-ray crystal structure of the protein A–Fc complex identifies the protein–protein interaction site and the specific interactions that are responsible

for binding.<sup>36</sup> In the crystal, fragment B of protein A forms two important contacts with the Fc domain, one is predominantly hydrophobic and the second is mainly polar. While our intention was not to directly mimic protein A–Fc binding, we anticipated that knowledge of the strength and location of this interaction would be helpful in analyzing the results of the NP binding studies (vide infra). To this end a competitive inhibition experiment between protein A and NP7 to the Fc domain of IgG under various buffer conditions was carried out. Figure 6 shows the experimental design and results of the

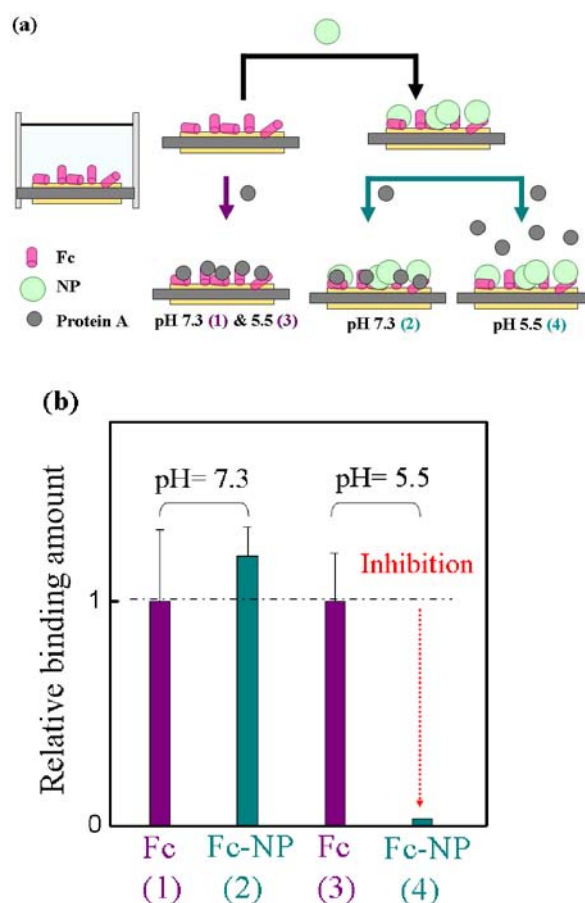


**Figure 6.** (a) Schematic of the competitive binding of protein A to Fc in the presence and absence of NP7. (b) The interaction of the Fc fragment and protein A at pH 7.3 and 5.5 in PBS (35 mM, without salt), respectively, following treatment with NP7. The arrow color in part a corresponds to the color of the column in part b. Cyan column: the frequency change resulting from protein A binding to the Fc domain in the presence of NP7 at pH 7.3 (2) and 5.5 (4), respectively. Purple column: control experiment under the same conditions omitting NPs at pH 7.3 (1) and 5.5 (3), respectively. Relative binding is defined by comparing the binding amount of the NP to that of protein A for the Fc domain. Standard deviations were calculated from three independent measurements.

competition at pH 7.3 and 5.5. The QCM cell surface was functionalized with Fc fragments. NPs were introduced into the cells at pH 5.5 and 7.3, respectively, until saturation of the signal was observed. Protein A was then injected into the cells and the response to the added protein was monitored. A control experiment was performed following the same procedure except the NPs were omitted. The results show that at pH 7.3, NP7 has little effect on protein A binding to the

Fc domain. In contrast, at pH 5.5, preincubation of the Fc domain with NP7 inhibits protein A binding (~97% inhibition, Figure 6b column 4). Nonspecific binding between NP7 and protein A at pH 7.3 and 5.5 was also considered. We attribute the difference in association between protein A and NP7 to the change in net charge of the NP/protein A binding domain of Fc due to the status of protonation of histidine residues (vide infra). Furthermore, the experimental results indicate that NP7 and protein A can compete for the same binding site at pH 5.5.

**NP7 Inhibition of Protein A Binding to IgG.** The preceding results suggest that NP7 competes with protein A at a discrete Fc domain at pH 5.5. To establish if this result is also observed with an intact IgG, a procedure similar to that described in Figure 6a was carried out only the Fc domain was replaced with IgG in the immobilization step (Experimental Methods, Supporting Information). NP7 was injected into the cell with immobilized IgG until signal saturation was observed. A solution of protein A was subsequently injected. The control experiment consisted of the same procedure except the addition of NPs was omitted. At pH 7.3, there was no difference between cells with or without NP7. The results are quite similar to the previous experiment with the Fc fragment, no inhibition (competition) between NP7 with protein A at pH 7.3. In contrast, at pH 5.5, there is little interaction between protein A and Fc after IgG was treated with NP7 (Figure 7, cyan, column

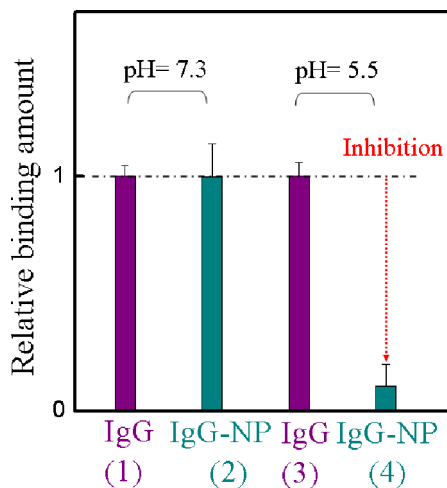


**Figure 7.** Interaction between the Fc fragment of IgG and protein A at pH 7.3 and 5.5 in 35 mM phosphate buffer, before and after addition of NP7. The experimental design is similar to Figure 6a. Whole IgG was used to functionalize the QCM cell. The color of the column in the graph corresponds to the color of the arrowhead in Figure 6a. Cyan column: the frequency change was caused by protein A binding to the Fc domain of IgG in the presence of NP7 at pH 7.3 (2) and 5.5 (4), respectively. Purple column: control experiment under the same conditions except omitting the introduction of NPs at pH 7.3 (1) and 5.5 (3). Relative binding is defined as comparing the binding amount of the NP to that of protein A for whole IgG. Standard deviations were calculated from three independent measurements.

4). We conclude that the NP inhibits protein A binding at pH 5.5. This phenomenon is analogous to the pH-dependent interaction of the neonatal Fc receptor (FcRn) to IgG.<sup>37–40</sup> It exhibits high-affinity binding at pH 6.0–6.5 but weaker binding at pH 7.0–7.5. FcRn binds maternal IgG from ingested milk in the gut (pH 6.0–6.5) and delivers it to the bloodstream of the newborn (pH 7.0–7.5). In a process, called transcytosis, IgG proteins are transported across the gut epithelium to enter the

bloodstream of the neonate. Many studies<sup>38–40</sup> have shown that the pH response is due to histidine residues on the Fc domain. Both the FcRn and protein A binding sites are at the interface between the CH<sub>2</sub>-CH<sub>3</sub> domains (vide infra) of IgG. It is also known that fragment B of protein A inhibits FcRn binding to IgG.<sup>41</sup> This indicates there is overlap in the binding domains of FcRn and protein A to the Fc domain of IgG. In addition, research has shown that two histidines<sup>39,41</sup> (Fc residues 310 and 433) are responsible for the pH-dependent binding, and they are also located on fragment B of the protein A–IgG binding interface. The similar pH response of NP7 and FcRn binding to the Fc domain supports the hypothesis that the pH dependence stems from interactions with His residues.

**Computational Study of the Fc Surface and Analysis of Potential NP7 Binding Sites.** To understand the origins of the inhibition of protein A–Fc binding by NP7, the binding surface of the protein A–Fc complex was analyzed from the X-ray crystal structure of the complex. The analysis identifies the protein–protein interaction site and the specific residues that are responsible for binding.<sup>36</sup> The interaction occurs in the hinge region between the CH<sub>2</sub> and CH<sub>3</sub> domains. Upon binding protein A, 660 Å<sup>2</sup> of SASA on Fc is covered. Figure 8 presents various views of the Fc dimer with the atoms involved in binding protein A shown in cyan (an atom in Fc was defined as in contact with protein A if it was within 5 Å of any heavy atom of protein A). The experimental structure of protein A bound to Fc (PDB ID 1FC2) was used to calculate the contacting atoms, and the images in Figure 8 were generated from the apo structure (PDB 1HZH) by using UCSF Chimera.<sup>42</sup> Using the 5 Å distance for defining contact, 77 heavy atoms in Fc are in contact with protein A. The interface between protein A and Fc is stabilized mainly by hydrophobic interactions, with relatively few polar contacts.<sup>18</sup> The hinge region between the CH<sub>2</sub> and CH<sub>3</sub> domains of Fc also contains ample polar groups allowing for high-affinity binding to biochemically diverse surfaces.

A computational study of the Fc surface was performed to search for likely NP7 binding regions to assist in interpreting the pH dependence of the protein A–NP competition study. In addition to hydrogen bond donor and acceptor groups, NP7 is composed of hydrophobic and negatively charged groups, thus, the Fc protein surface was scanned for complementary regions (hydrophobic and positively charged) as described in the Experimental Methods (Supporting Information). The calculated charge and hydrophobicity scores for all Fc residues are presented in Table S4 (Supporting Information). To distill the surface region calculations to a single value, the combined score of a surface region was defined as follows: 2 × charge score + hydrophobic score. The combined score was set to 0 for surface regions with charge score ≤ 0. The SASA, hydrophobic score, charge score, and combined score for all 97 surface regions are presented in Table S5 in the Supporting Information.

**Modeling of Potential NP7 Binding Sites at Neutral pH.** The surface region with the highest combined score (+8.8) at neutral pH is centered on Thr289 in the CH<sub>2</sub> domain of Fc. This region has SASA of 669 Å<sup>2</sup>, and it includes 5 positively charged residues (Lys274, Lys288, Lys290, Lys292, and Lys301) and only one negatively charged residue (Glu272), giving it a charge score of +4. The hydrophobicity score is +0.8 and the partially exposed hydrophobic residues in the region include the following: Phe275, Val284, Ala287, Val303, and Val305. Figure 9 depicts a view of the Fc dimer, highlighting the centers of the surface regions with the highest combined

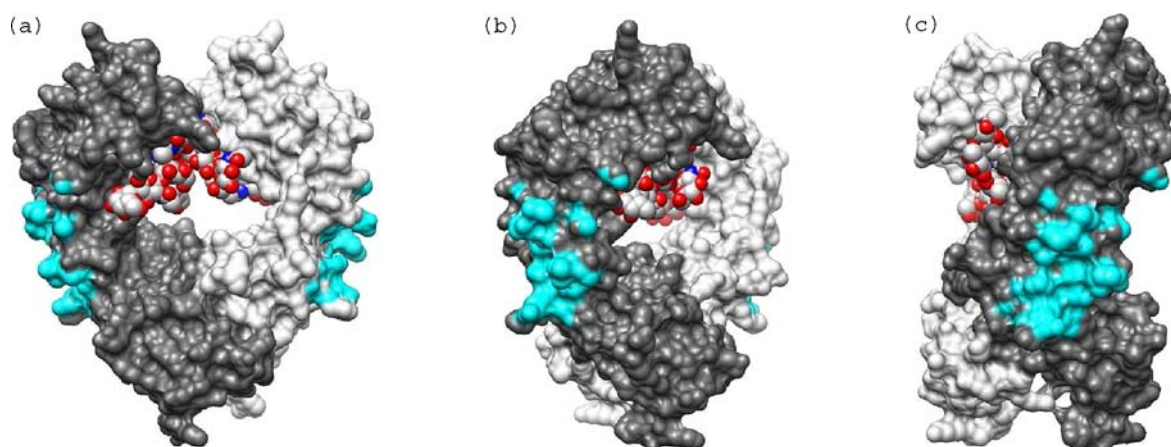


**Figure 8.** Protein A binding site shown on IgG1–Fc dimer. Binding site atoms are cyan. An Fc atom is considered in contact with protein A if it is within 5 Å of any heavy atom of protein A. The holo structure PDB ID 1FC2 was used to calculate distances between Fc and protein A. The N-terminus of Fc is at the top of the view and the C-terminus is at the bottom. Chain H is dark gray, chain K is light gray, and the carbohydrates bound in the Fc dimer core (red) are shown in the space filled representation. Images generated from PDB ID 1HZH with UCSF Chimera.<sup>42</sup> The view in part b is rotated 45° about the vertical axis with respect to the view in part a, and the view in part c is rotate 90° with respect to part a.

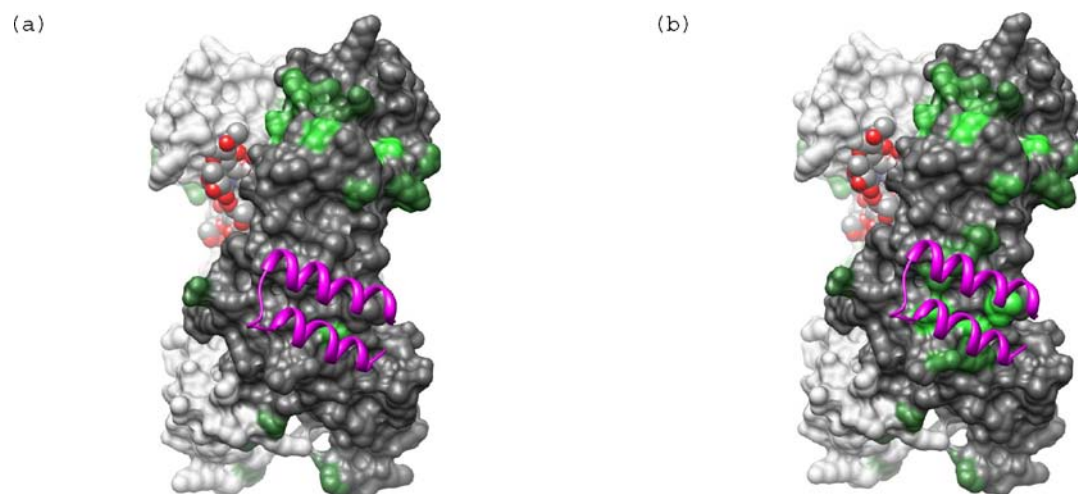


**Figure 9.** Computationally selected NP binding sites at (a) neutral and (b) low pH. Computational results indicate NP7 is more likely to bind the protein A binding site at lower pH in agreement with experimental observations. Residue side chains are green if the combined score of the surface region is greater than 0.0, and brighter shades of green indicate higher scores. (a) Results calculated assuming neutral pH and (b) at low pH where His residues can carry a positive charge. Chain H is dark gray, chain K is light gray, and the carbohydrates bound in the Fc dimer core are shown in space fill representation. Protein A appears as purple ribbons. Images generated from PDB ID 1HZH with UCSF Chimera.<sup>42</sup>

scores. Figure 9a depicts all surface regions with a combined score  $>0$  at neutral pH in green, with increased brightness corresponding to higher values. Notice that, in addition to the brightest green surface (Thr289), many other residues on the CH<sub>2</sub> domain are also green. It is likely that these residues in CH<sub>2</sub> form a contiguous interaction interface with NP7. These results indicate that protein A (shown as purple ribbons) and NP7 are unlikely to compete for the same binding site at neutral pH. This is consistent with the results of the inhibition study.

**Modeling of Potential NP7 Binding Sites at Low pH.** The surface region with the highest combined score (+9.4) at low pH is centered on Met252 in the hinge region between the CH<sub>2</sub> and CH<sub>3</sub> domains of Fc. This region has SASA of 812 Å<sup>2</sup>, and it includes 5 positively charged residues (Lys246, Lys248, Arg255, His310, and His435) and two negatively charged residues (Asp249 and Glu380), giving it a charge score of +3. The hydrophobicity score is +3.4 and exposed hydrophobic

surface includes the fully exposed side chain of Ile253 and the partially exposed side chains of Met252 and Leu314. Figure 9b depicts all surface regions with a combined score  $>0$  at low pH in green with increased brightness corresponding to higher values. The surface region centered on Met252 appears in bright green in the area covered by protein A. In addition to Met252, several other residues in the protein A binding region also appear in green. It is likely that these residues in the hinge region form a contiguous interaction interface with NP7. These results suggest that protein A and NP7 are likely to compete for the same binding site at lower pH and are consistent with the data obtained from the binding studies.

**Affinity of NP7 to the Fc Domain.** To calculate the binding affinity of IgG and NP7, IgG was immobilized on a QCM cell surface and NPs were injected in aliquots until signal saturation was achieved (Figure 10). A frequency change of approximately 3000 Hz was observed corresponding to almost complete coverage of the surface by NP7.<sup>43</sup> Washing the cells

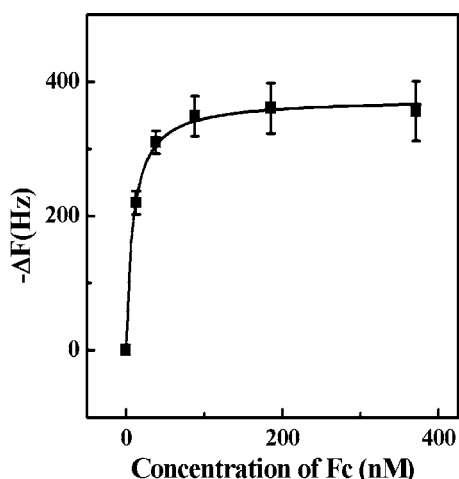


**Figure 10.** Binding isotherm of Fc domain to NP7 immobilized on QCM surface in water (pH 5.5). Standard deviations were calculated from three independent measurements.

resulted in a slight diminution of frequency (less than 2%). A solution of the Fc fragment was then added to the cells in aliquots and the resulting change in frequency was monitored. The data were fitted to a Langmuir isotherm from which a  $K_d$  of 8.5 nM for the NP–Fc fragment was obtained. A second method where the Fc fragment was immobilized was also used to obtain  $K_d$  (Figure S6, Supporting Information). The molecular weight of NP7 obtained by static light scattering is  $1.02 \times 10^4$  kDa (Figure S9, Supporting Information). A calculated apparent dissociation constant of 3.5 nM was obtained by nonlinear fitting of the binding isotherm to a Langmuir isotherm. The two dissociation constants measured by these independent experiments are in good agreement. The dissociation constant of protein A is  $10 \text{ nM}^{17}$  at pH 7. These results independently indicate that NP7 has a comparable affinity to IgG at pH 5.5 as protein A at pH 7. These results suggest that synthetic polymers with a composition of NP7 have the potential to be used as an affinity media for IgG.

## CONCLUSION

An iterative process was used to identify synthetic polymer NPs (50–65 nm) composed of 40% TBAm, 20% AAc, 2% Bis, and 38% NIPAm that binds to the Fc fragment of IgG. The binding was found to be pH sensitive. The binding amount of the synthetic polymer NPs to Fc at pH 5.5 is twice that at pH 7.3 in 20 mM phosphate buffer. The difference in binding is attributed to the difference in the charged state of histidine residues of Fc. At pH 5.5, NP7 can inhibit protein A binding to the Fc domain. However, there was no such competition observed at pH 7.3. A computational analysis identified potential binding domains. At pH 5.5, a binding domain of NP7 overlaps with the protein A–Fc binding domain. In addition, the affinity of NP7 at pH 5.5 is comparable to protein A at pH 7. We have also presented preliminary evidence that NP7 can capture the whole IgG. At pH 5.5, NP7 competes with the binding of protein A to IgG in a similar fashion to that of the Fc fragment. These results suggest that synthetic polymer NPs can be engineered to have an intrinsic affinity to a specific domain of a large biomacromolecule.

## ASSOCIATED CONTENT

### Supporting Information

Experimental methods for NPs preparation, confirmation of Fc–orientation immobilization, model calculation, competitive binding of protein A to Fc, and binding isotherm of NP 7 to the Fc. This material is available free of charge via the Internet at <http://pubs.acs.org>.

## AUTHOR INFORMATION

### Corresponding Author

[kjshea@uci.edu](mailto:kjshea@uci.edu)

### Notes

The authors declare no competing financial interest.

## ACKNOWLEDGMENTS

We are grateful for financial support from the NIH (NIH GM080506), The Shiseido Corp, MEXT (23111716), and JSPS (23750193). We also thank Initium, Inc. for QCM support. S.H.L. was supported by a National Science Council Taiwan graduate student study abroad fellowship. A.R. was supported by a NIH/NLM Pathway to Independence Award (K99LM010821); P.B. was supported by NIH grants LM010235-01A1 and 5T15LM007743. We also wish to thank Mr. Isao Yanagisawa (Shiseido).

## REFERENCES

- (1) Meenach, S. A.; Hilt, J. Z.; Anderson, K. W. *Acta Biomater.* **2010**, *6*, 1039–1046.
- (2) Bhojani, M. S.; Van Dort, M.; Rehemtulla, A.; Ross, B. D. *Mol. Pharmaceutics* **2010**, *7*, 1921–1929.
- (3) Tong, R.; Christian, D. A.; Tang, L.; Cabral, H.; Baker, J. R.; Kataoka, K.; Discher, D. E.; Cheng, J. J. *MRS Bull.* **2009**, *34*, 422–431.
- (4) Messerschmidt, S. K. E.; Musyanovych, A.; Altvater, M.; Scheurich, P.; Pfizenmaier, K.; Landfester, K.; Kontermann, R. E. *J. Controlled Release* **2009**, *137*, 69–77.
- (5) Davis, M. E.; Chen, Z.; Shin, D. M. *Nat. Rev. Drug Discovery* **2008**, *7*, 771–782.
- (6) Phillips, R. L.; Miranda, O. R.; You, C. C.; Rotello, V. M.; Bunz, U. H. F. *Angew. Chem., Int. Ed.* **2008**, *47*, 2590–2594.
- (7) You, C. C.; Miranda, O. R.; Gider, B.; Ghosh, P. S.; Kim, I. B.; Erdogan, B.; Krovi, S. A.; Bunz, U. H. F.; Rotello, V. M. *Nat. Nanotechnol.* **2007**, *2*, 318–323.
- (8) Horgan, A. M.; Moore, J. D.; Noble, J. E.; Worsley, G. J. *Trends Biotechnol.* **2010**, *28*, 485–494.
- (9) Hoshino, Y.; Urakami, T.; Kodama, T.; Koide, H.; Oku, N.; Okahata, Y.; Shea, K. J. *Small* **2009**, *5*, 1562–1568.
- (10) Hoshino, Y.; Koide, H.; Urakami, T.; Kanazawa, H.; Kodama, T.; Oku, N.; Shea, K. J. *J. Am. Chem. Soc.* **2010**, *132*, 6644–6645.
- (11) Hoshino, Y.; Koide, H.; Furuya, K.; Haberaecker, W. W.; Lee, S. H.; Kodama, T.; Kanazawa, H.; Oku, N.; Shea, K. J. *Proc. Natl. Acad. Sci. U.S.A.* **2012**, *109*, 33–38.
- (12) You, C. C.; De, M.; Han, G.; Rotello, V. M. *J. Am. Chem. Soc.* **2005**, *127*, 12873–12881.
- (13) Yoshimatsu, K.; Lesel, B. K.; Yonamine, Y.; Beierle, J. M.; Hoshino, Y.; Shea, K. J. *Angew. Chem., Int. Ed.* **2012**, *51*, 2455–2458.
- (14) <https://commonfund.nih.gov/proteincapture/>
- (15) Roque, A. C. A.; Silva, C. S. O.; Taipa, M. A. *J. Chromatogr., A* **2007**, *1160*, 44–55.
- (16) Miyakawa, S.; Nomura, Y.; Sakamoto, T.; Yamaguchi, Y.; Kato, K.; Yamazaki, S.; Nakamura, Y. *RNA* **2008**, *14*, 1154–1163.
- (17) DeLano, W. L.; Ultsch, M. H.; de Vos, A. M.; Wells, J. A. *Science* **2000**, *287*, 1279–1283.
- (18) Sauereriksson, A. E.; Kleywegt, G. J.; Uhlén, M.; Jones, T. A. *Structure* **1995**, *3*, 265–278.

- (19) (a) Chee, C. K.; Rimmer, S.; Soutar, I.; Swanson, L. *Polymer* **2001**, *42*, 5079–5087. (b) Ottaviani, M. F.; Winnik, F. M.; Bossmann, S. H.; Turro, N. J. *Helv. Chim. Acta* **2001**, *84*, 2476–2492.
- (20) Hoshino, Y.; Haberaecker, W. W.; Kodama, T.; Zeng, Z. Y.; Okahata, Y.; Shea, K. J. *J. Am. Chem. Soc.* **2010**, *132*, 13648–13650.
- (21) Roque, A. C. A.; Lowe, C. R.; Taipa, M. A. *Biotechnol. Prog.* **2004**, *20*, 639–654.
- (22) Low, D.; O'Leary, R.; Pujar, N. S. *J. Chromatogr., B: Anal. Technol. Biomed. Life Sci.* **2007**, *848*, 48–63.
- (23) Thommes, J.; Etzel, M. *Biotechnol. Prog.* **2007**, *23*, 42–45.
- (24) Nematollahzadeh, A.; Sun, W.; Aureliano, C. S. A.; Lutkemeyer, D.; Stute, J.; Abdekhodaie, M. J.; Shojaei, A.; Sellergren, B. *Angew. Chem., Int. Ed.* **2011**, *50*, 495–498.
- (25) Ren, L. B.; Liu, Z.; Liu, Y. C.; Dou, P.; Chen, H. Y. *Angew. Chem., Int. Ed.* **2009**, *48*, 6704–6707.
- (26) Debord, J. D.; Lyon, L. A. *Langmuir* **2003**, *19*, 7662–7664.
- (27) Ogawa, K.; Nakayama, A.; Kokufuta, E. *Langmuir* **2003**, *19*, 3178–3184.
- (28) Song, D.; Forciniti, D. *J. Colloid Interface Sci.* **2000**, *221*, 25–37.
- (29) Jans, H.; Liu, X.; Austin, L.; Maes, G.; Huo, Q. *Anal. Chem.* **2009**, *81*, 9425–9432.
- (30) Peppel, K.; Crawford, D.; Beutler, B. *J. Exp. Med.* **1991**, *174*, 1483–1489.
- (31) Goncalves, E.; Kitas, E.; Seelig, J. *Biochemistry* **2006**, *45*, 3086–3094.
- (32) Lin, F. Y.; Chen, C. S.; Chen, W. Y.; Yamamoto, S. *J. Chromatogr., A* **2001**, *912*, 281–289.
- (33) Zhang, S. P.; Sun, Y. *Biotechnol. Bioeng.* **2001**, *75*, 710–717.
- (34) De, M.; You, C. C.; Srivastava, S.; Rotello, V. M. *J. Am. Chem. Soc.* **2007**, *129*, 10747–10753.
- (35) Zeng, Z. Y.; Patel, J.; Lee, S. H.; McCallum, M.; Tyagi, A.; Yan, M. D.; Shea, K. J. *J. Am. Chem. Soc.* **2012**, *134*, 2681–2690.
- (36) Deisenhofer, J. *Biochemistry* **1981**, *20*, 2361–2370.
- (37) Raghavan, M.; Bjorkman, P. J. *Annu. Rev. Cell Dev. Biol.* **1996**, *12*, 181–220.
- (38) Kim, J. K.; Tsen, M. F.; Ghetie, V.; Ward, E. S. *Eur. J. Immunol.* **1994**, *24*, 2429–2434.
- (39) Raghavan, M.; Bonagura, V. R.; Morrison, S. L.; Bjorkman, P. J. *Biochemistry* **1995**, *34*, 14649–14657.
- (40) Martin, W. L.; West, A. P.; Gan, L.; Bjorkman, P. J. *Mol. Cell* **2001**, *7*, 867–877.
- (41) Raghavan, M.; Chen, M. Y.; Gastinel, L. N.; Bjorkman, P. J. *Immunity* **1994**, *1*, 303–315.
- (42) Pettersen, E. F.; Goddard, T. D.; Huang, C. C.; Couch, G. S.; Greenblatt, D. M.; Meng, E. C.; Ferrin, T. E. *J. Comput. Chem.* **2004**, *25*, 1605–1612.
- (43) Ozeki, T.; Morita, M.; Yoshimine, H.; Furusawa, H.; Okahata, Y. *Anal. Chem.* **2007**, *79*, 79–88.